ORIGINAL PAPER

On the Investigations of Resilient Modulus of Residual Tropical Gravel Lateritic Soils from Senegal (West Africa)

**Meissa Fall · Auckpath Sawangsuriya ·
Craig H. Benson · Tuncer B. Edil ·
Peter J. Bosscher**

Abstract Investigations on the mechanical behavior of compacted gravel lateritic soils have been the subject of several studies. Used as road materials, soils tests were mainly performed using standard tests. Static loads as unconfined compression test (UCT) remain the only engineering approach used. Alternative testing techniques can be chosen as supplementary tests for characterizing pavement materials. These researches were conducted so as to determine the response of these particular and problematic soils in its compacted form with road traffic loads. This paper presents the results of research conducted to investigate the effect of the soil compacity on the resilient modulus of lateritic soils. The influence of the percentage of cement added so as to stabilize each sample at the optimum modified proctor (OPM) State was also determined. Soil big specimens of around 180 mm diameter (with length to diameter aspect ratio of 2:1) were prepared according to the standard procedure described by AASHTO T 307 and then were subjected to repeated load triaxial tests. The models used, analyzed and developed in this paper are mainly the Andrei and the Uzan–Witczak universal model. Test results showed that the specimen compacity has no significant influence on the resilient modulus of the investigated gravel lateritic soils. Soil specimens with variation of the percentage of cement added exhibited the highest resilient modulus values while the specimens with variation of the compacity exhibited the lowest values. The resilient modulus variation seems to be independent of the level of stress.

Keywords Lateritic soils · Compaction ·
Unconfining compression tests · Triaxial tests ·
Optimum modified proctor · Resilient modulus ·
Road design · Geotechnical engineering ·
AASHTO · NCHRP

M. Fall (✉)
Faculty of Sciences and Techniques, Earth Sciences Institute, University Cheikh Anta Diop, BP 15 685 Dakar-Fann, Dakar, Senegal
e-mail: meissaf@ucad.sn

A. Sawangsuriya · C. H. Benson · T. B. Edil ·
P. J. Bosscher
Department of Civil and Environmental Engineering, University of Wisconsin-Madison, Madison, WI 53706, USA

1 Introduction

Previous studies (Fall 1993; Fall and Tisot 1994, 1995, 1996; Fall et al. 2002a, b) underlined the importance to have adequate characteristics for an optimal design of road structures in tropical African regions. Researches in Senegal during the last 20 years permits to pronounce now amply on the geotechnical reasons of the premature ruin of road structures designed with tropical lateritic soils. The main problem of the weak life span of the road

structures is due to an under-estimated engineering design caused by the use of inappropriate characteristics with no controls in the numerical codes of road design. In situ investigations done since then with complementary experimental works, permits to have reliable engineering information on local subgrades, the most common gravel lateritic materials, road making aggregates and finally the laterite-cement (lateritic soils stabilized with 1–3% of cement). This last material was the subject of particular attention, due to its specificity and especially to the fact that all bases or sub-bases layers in the African Western Countries is prepared with. Finally, a fine analysis of the interrelationships between these features, their strength parameters and their modulus of elasticity permits to have now tools of choice to do reasonable road design. The issue is therefore to define new norms/standards and specifications in road geotechnique.

In Senegal, as in a lot of developing countries, road construction is done without norms and standards. Road design had never been based on realistic knowledge or objectives information of local materials characteristics, the gravel lateritic soil notably. Indeed, the very scattered values of the elastic parameters of the materials, among others the dynamic modulus in technical reports can constitute a factor to convince of it. Besides, most base layers treated by cement undergo intense deformation or arrive at a premature failure. It probably leads us to think about the methods of design utilized. Is it that the empirical design methods, as, among others, the method of the BCEOM-CEBTP (1984) mostly used or the CBR methods, are the most suitable for gravel lateritic soils design of the bases pavements treated by cement? Is it necessary to incriminate the in situ setting of the laterite-cement? Do these methods say rational otherwise of road design that adopt analytic techniques and use numerical codes of calculation, are very sensitive to the value of the input parameters (Fall et al. 2002a, b)? If the so-called rational methods are adopted, what justifies that for laterites of CBR lower to 80% and stabilized with cement added at 2.5 or 3%, the very scattered values of elastic modulus ranging from 15,000 to 23,000 bars (and even sometimes 50,000 bars). It can be said therefore that in Senegal, regarding road studies, there are no serious specifications. In this paper, we'll present investigations on monotonic (unconfined compression tests (UCT)) and cyclic loads (resilient modulus tests) of

lateritic soils from Senegal and the results obtained are very different to those obtained since then in the mechanic characteristics of these soils.

2 Topics

The soil and aggregate layers forming the foundation of pavements or highway pavements are subjected to repeated traffic loading. Under individual cycles of loading, the layers behave essentially elastically, while plastic deformation accumulates with repeated cycles. Design of pavements requires a significant amount of input data such as traffic loading characteristics, properties of materials (base, subbase, and subgrade soil), environmental conditions and construction procedures. Properties of base materials are often evaluated by laboratory tests such as California bearing ratio (CBR), which do not represent the nature of repeated dynamic traffic load on subgrade soil. Recognizing this deficiency, the AASHTO guide for design of pavement structures (1986 and 1993) and the 2002 AASHTO guide for the design of new and rehabilitated pavement structures incorporated the resilient modulus for characterizing subgrade soils in flexible pavement design.

Resilient modulus is usually determined by repeated load triaxial tests with constant confining pressure, σ_3, and with the deviator stress cycled between the hydrostatic state and some positive deviator stress ($\sigma_1 - \sigma_3$). Resilient modulus (M_R) as defined is equivalent to resilient Young's modulus (E_R). Resilient modulus of subgrade soils can be determined by laboratory testing such as the repeated load triaxial test. The AASHTO T 307 (determining the resilient modulus of soils and aggregate materials) is the current standard procedure designated by AASHTO for determining the resilient modulus of subgrade soils using the repeated load triaxial test. According to this standard procedure, the specimen size (diameter and length) depends upon the soil type as classified from particle size analysis and consistency limits. In addition, for type 2 materials (fine-grained soils), compacted specimens should be prepared in a mold that will produce a specimen of minimum diameter equals to five times the maximum particle size with an aspect ratio of length to diameter of not less than 2:1.

From an engineering point of view, there is much to be desired about a mechanistic approach to pavement design. Recall that "mechanistic" means that the principles of engineering mechanics will apply, i.e., the design process will be rational (NCHRP 2004). Yoder and Witczak (1975) point out that for any pavement design procedure to be completely rational in nature: three elements must be fully considered. These are (1) the theory used to predict the assumed failure or distress parameter, (2) the evaluation of the materials properties applicable to the selected theory, and (3) the determination of the relationship between the magnitude of the parameter in question to the performance level desired (NCHRP 2004). While this Guide will consider all three elements only the first is discussed in this overview.

Generally for the general concept of a multi-layered elastic system, the analytical solution to the state of stress or strain makes several assumptions. Some of these are (1) the material properties of each layer are homogeneous; that is, the properties at each point are the same; (2) each layer has a finite thickness except for the lower layer, and all are infinite in the lateral directions. Other assumption are, (3) each layer is isotropic; that is, the property at a specific point is the same in every direction or orientation, (4) full friction is developed between layers at each interface. Finally, (5) surface shearing forces are not present at the surface, and (6) the stress solutions are characterized by two material properties for each layer. These properties are Poisson's ratio, μ and the elastic modulus E.

Yoder and Witczak (1975) continue to show that at a given point within any layer, static equilibrium requires that nine stresses exist. These stresses are comprised of three normal stresses (σ_z, σ_r, σ_t) acting perpendicular to the element faces and six shearing stresses (τ_{rt}, τ_{tr}, τ_{rz}, τ_{zr}, τ_{tz}, τ_{zt}) acting parallel to the faces. Static equilibrium conditions also show that the shear stresses acting on intersecting faces are equal. Thus, $\tau_{rz} = \tau_{zr}$, $\tau_{rt} = \tau_{tr}$, and $\tau_{tz} = \tau_{zt}$. At each point in the system, there exists a certain orientation of the element such that the shear stresses acting on each face are zero. The normal stresses under this condition are defined as principal stresses and are denoted by σ_z (major stress), σ_r (intermediate), and σ_t (minor). The sum of the principal stresses at a point is defined as the bulk stress (θ). Considering this triaxial stress state of any element, the strains (for the vertical, radial, and tangential directions, respectively) may be determined from the following equations:

$$\varepsilon_z = \frac{1}{E}[\sigma_z - \mu(\sigma_r - \sigma_t)]$$

$$\varepsilon_r = \frac{1}{E}[\sigma_z - \mu(\sigma_t + \sigma_r)]$$

$$\varepsilon_t = \frac{1}{E}[\sigma_t - \mu(\sigma_r - \sigma_z)].$$

Building on these general equations, the type of theory used is generally distinguished by three properties of the material behavior response. They are the relationship between stress and strain (linear or nonlinear), the time dependency of strain under a constant stress level (viscous or non-viscous), and the degree to which the material can rebound or recover strain after stress removal (plastic or elastic). All three properties are to be addressed in the guide as appropriate to the various paving materials. Much of the "empirical" part of mechanistic-empirical relates to the characterization of materials or to various traffic, environmental or other inputs to the design process.

Generally, flexible and rigid pavements respond to loads in such different ways that there are fundamental differences in the analysis theories applied. Basically, rigid pavement slabs are cases where non-linearity of the stress–strain relationship is not an issue while discontinuities such as cracks and joints are of major importance. Essentially, the opposite is true with flexible pavements, i.e., non-linearity of the stress–strain relationship is a major issue while discontinuities are secondary or non-existent. Rehabilitated pavements, especially those with a combination of rigid and flexible layers, are an entirely different class and are to be handled separately in the Guide.

While the mechanistic approach to pavement design and analysis is much more rational than the empirical, it also is much more technically demanding. As mentioned earlier, mechanistic-empirical procedures were not practical until the advent of high-speed computers. The reason is the computational demands associated with the differential equations and finite element matrix solutions employed by the various analysis models. Such models will be incorporated in and described in detail in the Guide. As will be noted in the model descriptions, the choice of a model and how it is applied often will relate to the computational requirements and how much time is required to accomplish those computations.

3 Nonlinear Resilient Modulus Model

The resilient modulus, defined as the unloading modulus after many cycles of repeated loading, is used in pavement engineering as an appropriate measure of stiffness for the layers in a pavement structure. The sample is initially subjected to a hydrostatic confining pressure σ_c, which induces an initial strain ε_c (unmeasured in the test, but the same in all directions for isotropic material behavior). The axial stress is then cycled at a constant magnitude $\Delta\sigma$, which induces the cyclic resilient axial strain $\Delta\varepsilon$. The resilient modulus M_R is defined simply as the ratio of the cyclic axial stress to resilient axial strain:

$$M_R = \frac{\Delta\sigma}{\Delta\varepsilon}.$$

The resilient modulus for most pavement materials is stress dependent. Many nonlinear models have been proposed over the years for incorporating the effects of stress level on the resilient modulus. A general form for these models can be expressed as (Andrei 1999):

$$M_R = k_1 P_a \left(\frac{\theta - 3k_6}{P_a}\right)^{k_2} \left(\frac{\tau_{oct}}{P_a} + k_7\right)^{k_3}$$

in which

M_R = resilient modulus
θ = bulk stress at the peak of the loading
$= \sigma_x + \sigma_y + \sigma_z$
$= 3\sigma_c + \Delta\sigma$, for standard triaxial compression loading
τ_{oct} = octahedral shear stress at the peak of the loading

$$= \left\{\frac{1}{9}[(\sigma_y - \sigma_y)^2 + (\sigma_y - \sigma_z)^2 + (\sigma_z - \sigma_x)^2] + \frac{2}{3}\left[\tau_{xy}^2 + \tau_{yz}^2 + \tau_{zx}^2\right]\right\}^{1/2}$$

$$= \frac{\sqrt{2}}{3}\Delta\sigma$$

$= \Delta\sigma$ for standard triaxial compression loading
P_a = atmospheric pressure (normalizing factor)

$k_1 - k_7$ = material parameters subject to the following constraints:
$k_1 > 0; k_2 > 0; k_3 < 0; k_6 < 0; k_7 > 1$

A simplified version of the Andrei equation with $k_6 = 0$ and $k_7 = 1$ has been adopted and gives the following equation:

$$M_R = k_1 P_a \left(\frac{\theta}{P_a}\right)^{k_2} \left(\frac{\tau_{oct}}{P_a} + 1\right)^{k_3}$$

The Andrei equation combines both the stiffening effect of bulk stress (the term under the k_2 exponent) and the softening effect of shear stress (the term under the k_3 exponent). Through appropriate choices of the material parameters $k_1 - k_7$, one can recover the familiar two-parameter bulk stress model for granular materials and its companion two-parameter shear stress model for cohesive soils, the Uzan–Witczak universal model (Witczak and Uzan 1988), and the $k_1 - k_6$ model from the Strategic Highway Research Program's (SHRP) flexible pavement performance models (Lytton et al. 1993). The Andrei equation and its various specializations are convenient functional forms for fitting laboratory resilient modulus test data.

4 Experimental Program and Results

The soils considered in this study were collected from different locations within Senegal (West Africa). Standard laboratory tests were conducted to classify these soils and determine their properties. Laboratory testing consisted of particle size analysis (mechanical sieving and hydrometer analysis), specific gravity, consistency limits, and modified proctor compaction test. Moreover, the repeated load triaxial test was used to determine the resilient modulus of these soils.

4.1 Soil Properties

Laboratory tests were conducted on the investigated soils following the standard procedures of the American society for testing and materials (ASTM). The Modified Proctor compaction test was conducted using the AASHTO T 99 procedure. Table 1 present a summary of test results. Test results showed that the

Table 1 Properties of investigated soils

	LL (%)	PL (%)	PI (%)	% < 20 mm (gravel)	%<2 mm (sand)	%<80 μm (fines)	γ_{max} (kN/m³)	W_{opt} (%)	$\gamma_{d\ max}$ (kN/m³)	CBR at 95% OPM (%)	GI	AASHTO
	Characteristics before and after CBR test											
Lat.1 Sindia	38.2–	22.8–	15.4–	77–95	22–54	10/16	22.6	11.7	20.20	60	4	A2–6
Lat. 2 Mont Rolland	39.8–38.8	20.8–18.5	19–20.3	90–100	20–30	8/14	23.2	11.7	20.78	84	7	A2–6
Lat. 3 Colonat	32.5–28.5	16.3–14.8	16.2–13.7	95–100	16–22	12/10	23.2	6.1	21.87	84	5	A2–6
Lat.4 Kamacounda	38.2–36.2	20–19.5	18.2–16.7	98–100	35–46	20/22	22.0	11.7	19.65	67	5	A2–6
Lat.5 Oudoukar	37.7–34.2	19–17.5	18.7–16.7	95–100	32–42	14/18	21.9	9.0	20.10	74	6	A2–6
Lat.6 Soumbourou Pakao	32.1–	15.3–	16.8–	80–	–	16/–	21.8	7.5	20.30	68	5	A2–6

LL, liquid limit; PL, plastic limit; PI, plasticity index; w_{opt}, optimum moisture content; $\gamma_{d\ max}$, maximum dry unit weight; GI, group index

selected soils are classified mainly as A-26 materials according to AASHTO.

4.2 Unconfined Compression Test

Preparation and testing of soil specimens were conducted in accordance with AASHTO T 208-70. All soil samples were prepared under the optimum moisture content and maximum dry unit weight. This test had been done so as to have reliable correlation with the CBR values. It permits to have a comparison with the ancient correlations made in Senegal with an UCT test.

4.3 Repeated Load Triaxial Test

Preparation and testing of soil specimens were conducted in accordance with AASHTO T 307. The test sequence required for these kinds of soils is the one specified by the procedure AASHTOO T 292-97. All soil samples were prepared under the optimum moisture content and maximum dry unit weight.

5 Alternative Testing Techniques for Modulus

Stiffness measurements have gained increased appreciation in pavement engineering. Bender elements (BE) and soil stiffness gauge (SSG) have been adopted as they show potential and means of monitoring the stiffness and/or modulus of pavement materials. The typical range of strain amplitudes imposed by the bender elements and the SSG is compared with those incurred in the pavement base and subgrade layers to evaluate their suitability in the assessment of pavement layer stiffness and/or modulus (Fig. 1 and Table 2) (Sawangsuriya et al. 2003).

The strains induced in the pavement bases and subgrades that are subjected to the typical traffic loadings were compiled from other studies. In general, they can be classified into three main groups: (1) finite-element analysis, (2) large-scale model experiment, and (3) in situ test section. Table 2 presents the vertical strains in base, subbase, and subgrade layers summarized from various studies. The type of measurement and/or analysis, pavement structure, and loading characteristic employed in each study are also reported herein.
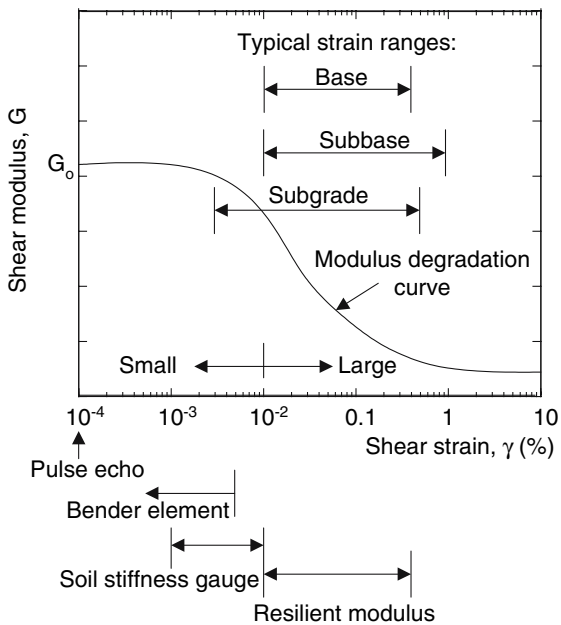
Fig. 1 Typical variation in shear modulus with various shear strain levels

For pavement bases and subgrades, the stress–strain behavior of soil is highly nonlinear and soil modulus may decay with strain by orders of magnitude. A relationship between the small-strain (linear-elastic) modulus (strains less than 10^{-2}%) and nonlinear behavior exhibited by soils at large strains (above 10^{-2}%) must be established. The shear modulus of soil at various shear strain levels for different pavement layers and modulus tests is shown in Fig. 1. Generally, strains in base and subbase vary from 0.01% to 1%, whereas those in subgrade may vary from 0.003% to 0.6%. Therefore, the pavement base, subbase, and subgrade layers involve strains at higher levels, i.e., typical strain range of 10^{-2}% to 1%, and soil exhibits nonlinear properties. Figure 1 also shows that the resilient modulus (M_r) test operates within these strain range.

We present below some results derived from UCT known as part of the only means used in some tropical countries to evaluate the soil stiffness and also the results of bender elements tests so as to make a comparison of these results with models given by the resilient modulus tests.

5.1 Unconfined Compression Tests

As seen from the tables below (Table 3a–e), we can evaluate that these results are mainly different to

those obtained since then in Senegal (Fall et al. 2002a, b) and from different African laboratories. The UC modulus (E_s; s means static) is less than 300 MPa for the samples stabilized by cement. It was generally admitted that the static modulus used for road design purposes and for materials with nearly 2–3% of cement, that the soil rigidity exceeds 1,000 MPA. The general trend is often the same for all the samples, from 95% of compaction at the OPM to 100%, we can easily admit than the soil rigidity increase as attested by the Table 3a–e. And, also the modulus increase at the same manner from 1% to 3% of cement added in the soil samples. The soil rigidity seems to be more affected by the variation of the percentage of cement added so as to stabilize the soil samples tested.

As seen in the tables below, the soil compacity do not makes significant difference when the samples are tested at 100% of the maximum density, excepted to 90% and 95% of the compacity where the difference can be noticed from sample to sample in regard to the soil's physical characteristics. Nevertheless, the state of reference remains the soil at 100% of compacity, which is the reference of soil settings in situ.

5.2 Bender Elements

An elastic wave propagation technique that utilizes two-layer piezoceramic bender elements as source and receiver provides a means of measuring the shear wave velocity and the corresponding small-strain shear modulus. The bender element test has become increasingly popular in a variety of geotechnical laboratory applications (Dyvik and Madshus 1985; Thomann and Hryciw 1990; Souto et al. 1994; Fam and Santamarina 1995; Zeng and Ni 1998; Fioravante and Capoferri 2001; Pennington et al. 2001; Mancuso et al. 2002). The transmitting bender element produces a shear wave (S-wave), which propagates through the soil when it is excited by an applied voltage signal. This S-wave impinges on the receiving bender element, causing it to bend, which in turn produces a very small voltage signal. Figure 2a illustrates typical input and output signals from the transmitting and receiving bender elements.

In general, the signals may be different from those in Fig. 2, possibly due to the stiffness of the soil, the boundary conditions, the test apparatus, the degree of fixity of the bender element into the platen or housing,

Table 2 Vertical strains in base, subbase, and subgrade layers

References	Method of estimating strain	Type of measurement and/or analysis	Pavement structure	Loading characteristic	Vertical strain (%)		
					Base	Subbase	Subgrade
Brown and Pappin (1981)	2D finite-element analysis	Nonlinear	50-mm surface 170-mm base Subgrade	8-kN wheel load 530-kPa contact pressure	0.15	NA	0.12–0.18
Chen et al. (1986)	3D finite-element analysis	Linear elastic	38-mm, 50-mm, 76-mm and 100-mm surface 200-mm base 4293-mm subgrade	20-kN and 24-kN wheel loads 518-kPa, 621-kPa and 759-kPa contact pressures	NA	NA	0.035–0.074
Hardy and Cebon (1993)	Test section	LVDTs	150-mm surface 300-mm base 914-mm subgrade	Four-axle vehicle: 29.1-kN steering axle, 40.4-kN-drive axial, 37.9-kN trailer's tandem axle group Speed: 50 and 80 km/h	NA	NA	0.04–0.07
Marsh and Jewell (1994)	Test section	Vertical strain transducers	30-mm surface 75-mm base 250-mm subbase 400-mm subgrade	553-kPa and 725-kPa contact pressures	NA	NA	7×10^{-3}–0.012
Chen et al. (1995)	2D and 3D finite-element analysis Multilayered elastic-based program	Linear and nonlinear	76-mm, 152-mm and 229-mm surface 305-mm base Subgrade	40.5 kN wheel load 689 kPa contact pressure	NA	NA	0.013–0.13
Pidwerbesky (1995)	Large-scale model experiment	Strain coil sensors	25-mm, 35-mm and 85-mm surface 135-mm, 200-mm and 300-mm base 200-mm subgrade	21-kN, 31-kN, 40-kN and 46-kN wheel load 550-kPa, 700-kPa and 825-kPa contact pressures	0.09–0.32	NA	0.09–0.35

Table 2 continued

References	Method of estimating strain	Type of measurement and/or analysis	Pavement structure	Loading characteristic	Vertical strain (%)		
					Base	Subbase	Subgrade
Dai and Van Deusen (1998)	Test section	LVDTs	127-mm and 200-mm surface 305-mm, 460-mm and 710-mm base 2690-mm, 2940-mm and 3168-mm subgrade	Five-axle tractor-trailer: 53.4-kN steering axle, 75.2-kN front axle, 73.9-kN back axle, 69.4-kN front axle and 81.9-kN back axle of tractor tandem Speed: 16–78 km/h	NA	NA	1.9×10^{-3}–0.019
Helwany et al. (1998)	2D and 3D finite-element analysis	Linear and nonlinear	150-mm surface-250-mm base 650-mm subbase Subgrade	90-kN axle load (45-kN wheel load) 550-kPa contact pressure	NA	0.012–0.058	NA
Saleh et al. (2003)	Large-scale model experiment	Strain coil sensors	25-mm surface 275-mm base- 1200-mm subgrade	- 40-kN, 50-kN and 60-kN wheel loads- 650-kPa, 700-kPa, 750-kPa, 800-kPa and 850-kPa contact pressures Speed: 6 km/h	0.02–0.13	NA	0.09–0.35
Tanyu et al. (2003)	Multilayered elastic-based program	Linear and nonlinear	125-mm surface 255-mm base 220-mm to 900-mm subbase 450-mm subgrade	35-kN wheel load 700-kPa contact pressure	NA	0.036–0.77	NA
Tutumluer et al. (2003)	Large-scale model experiment 2D finite-element analysis	Strain coil sensors Linear and nonlinear Isotropic and anisotropic	89-mm surface 203-mm base 1270-mm subgrade	28.9-kN wheel load 689-kPa contact pressure	0.011–0.062	NA	0.175–0.25

Table 2 continued

References	Method of estimating strain	Type of measurement and/or analysis	Pavement structure	Loading characteristic	Vertical strain (%)		
					Base	Subbase	Subgrade
de Pont et al. (2004)	Large-scale model experiment	Strain coil sensors	85-mm surface, 200-mm base, Subgrade	98-kN axle load (49-kN wheel load), Speed: 45 km/h	0.06–0.21	NA	0.15–0.31
Huang (2004)	Multilayered elastic-based program	Linear elastic	25-mm to 203-mm surface, 102-mm to 406-mm base, Subgrade	80-kN axle load (40-kN wheel load), 690-kPa contact pressure	NA	NA	0.025–0.4

and the size of the bender element and specimen (Sawangsuriya et al. 2003). By measuring the travel time of the S-wave and the tip-to-tip distance between transmitting and receiving bender elements, the S-wave velocity of the soil is obtained. The small-strain shear modulus (G) can be calculated according to elastic theory using the measured S-wave velocity (V_S) and total density of the soil (ρ) with the relationship $G = \rho v_s^2$ and $G = E_s/(2(1 + v))$ (with E_s, the static modulus; v, the Poisson's ratio).

A bender element test was performed on a specimen nearly 100 mm in diameter and nearly 180 mm high subjected to a range of confining pressures. Figure 2b shows the plot of shear modulus obtained from the bender element (BE) tests as a function of the compacity. Results (Fig. 3, Table 4a, b) indicated good agreement with those suggested by the UCT results.

6 Determination of Resilient Modulus

The repeated load triaxial test consists of applying a cyclic deviator stress (σ_d) on a cylindrical sample under constant confining pressure (σ_3) and measuring the recoverable axial strain (ε_r). The repeated axial load is applied in fixed 1 s cycles in which 0.1 s is the load duration (AASHTO Designation, T 292-97 2000). The specimen is first subjected to a minimum of 1,000 conditioning cycles to eliminate permanent deformation (Table 5).

Resilient modulus determined from the repeated load triaxial tests is defined as the ratio of the repeated axial deviator stress to the recoverable or resilient axial strain. Equation below shows the definition of the resilient modulus.

$$M_r = \frac{\sigma_d}{\varepsilon_r}.$$

The results of repeated load triaxial test Senegalese soils are presented in Tables 6 and 7, respectively. The test results of all the lateritic soils samples are presented in graphical format. Figures 1–3 show the variation of the resilient modulus of the specimens with the deviator stress, the bulk modulus and the bulk stress at different confining pressures, compacities and the percentage of cement added. The different soils preparations were conducted so as to obtain different specimens

Table 3 Unconfined compression test results

|	Strain at peak (%)	Elongation at peak (cm)	Load at offset yield (kN)	Modulus (kPa)	Peak load (kN)
a					
Lat1_100	2.968	0.51	2,050,844	24,159	2,633,014
Lat1_95	3.218	0.57	4,055,377	45,264	6,063,999
Lat1_95-bis[a]	2.431	0.44	966,768	14,382	1,123,007
Lat1_90	3.143	0.55	1,723,744	21,636	1,857,644
Lat1_1C-bis	3.262	0.59	2,781,331	40,010	3,405,238
Lat1_2C	3.613	0.68	6,364,552	90,046	8,001,880
b					
Lat3_100	0.978	0.17	2,014,600	51,918	2,050,101
Lat3_100-bis	2.468	0.45	875,117	7,205	891,535
Lat3_95	1.709	0.30	1,713,589	24,021	1,713,589
Lat3_95-bis	2.736	0.51	943,713	11,707	1,412,493
Lat3_90	2.933	0.53	984,787	15,589	1,207,621
Lat3_1C	3.591	0.66	655,428	13,796	2,091,719
Lat3_3C	1.995	0.39	8,997,565	113,136	9,220,573
Lat3_2C	3.323	0.64	4,885,669	71,912	8,805,998
c					
Lat4_100	2.303	0.42	2,903,733	40,334	3,142,615
Lat4_95	1.598	0.29	2,788,057	43,168	3,155,889
Lat4_95[a]	2.979	0.55	1,327,705	20,153	2,248,047
Lat4_95-bis	4.202	0.77	2,380,546	19,519	2,413,329
Lat4_90	1.897	0.34	2,855,220	61,363	3,038,465
Lat4_1C	2.162	0.40	2,500,572	48,980	2,931,707
Lat4_2C	2.656	0.50	6,499,368	118,514	9,042,475
Lat4_3C	2.203	0.44	42,449,632	203,726	16,476,059
d					
Lat5_100	2.299	0.41	1,770,544	24,642	2,151,503
Lat5_100	1.322	0.23	2,489,559	52,931	2,506,093
Lat5_95	3.184	0.55	1,969,806	12,686	1,975,900
Lat5_95-bis	3.08	0.54	1,254,790	14,934	1,815,853
Lat5_90	3.282	0.57	958,129	14,700	2,039,572
Lat5_1C	3.507	0.64	3,944,216	39,941	5,383,425
Lat5_2C	1.92	0.35	13,566,459	169,977	14,248,807
Lat5_3C	2.574	0.49	19,710,637	274,736	22,478,525
e					
Lat6_100	4.023	0.68	953,009	11,266	1,663,159
Lat6_95	2.62	0.43	1,851,007	16,816	1,855,527
Lat6_95-bis	5.416	0.78	875,032	7,688	1,042,169
Lat6_90	2.698	0.47	1,172,182	12,548	1,420,442
Lat6_1C	2.223	0.40	4,036,152	40,038	4,187,187
Lat6_2C	2.764	0.50	9,904,175	103,228	9,933,356
Lat6_3C	2.353	0.45	16,951,333	171,521	17,108,004

[a] Tests had been repeated
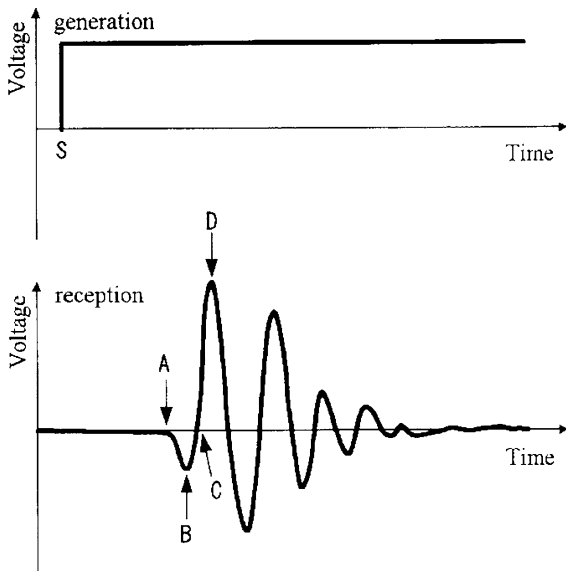
Fig. 2 Typical input and output signals from the transmitting and receiving bender elements
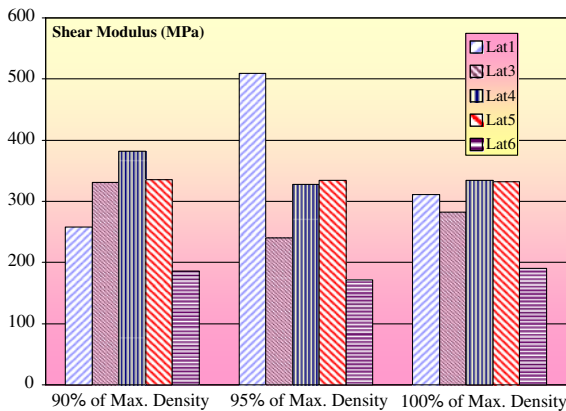
Fig. 3 Variation of the shear modulus with various soil samples' compacity

varying from 100% of the optimum modified proctor (i.e., 100 OPM) to 95% OPM and 90% OPM. The percentages of cement vary also from 1%, 2% and 3%. These particular conditions of soil preparation are those accepted in the field, the most bases layers in tropical regions are stabilized from 1% to 2% so as to increase the soil modulus and prevent the base layer to be ruined by the water effect.

The results of repeated load triaxial test on lateritic soils Lat.1 to Lat.6 are presented in Figs. 4a, b–8a, b respectively. In regard of the large amount of data, we have chosen to present all of the figures so as to show the results and to interpret them all. Figures

show the variation of the resilient modulus of Senegalese lateritic soils samples with the deviator stress or the bulk stress at different confining pressures, the sample's size remain the same.

As presented in the figures, the resilient modulus of the lateritic soils vary with deviator stress from 300 to 1,800 kPa for the specimen stabilized with 1% of cement; from 500 to 2,500 kPa at 2% of cement and greater at 3% of cement. The samples varying with the compacity (none stabilized) described trends, which are located under those ones stabilized by cement added and the soil moduli are less. The variation shows an increasing trend in the resilient modulus with the increase in the sample state of compaction and also the percentage of cement added for the same deviator stress. This increase is significant. In addition, the variation is independent of the level of the deviator stress, at low or high stress levels the behavior is the same.

Examination of all test result presented in Tables 4 and 5 indicates that the specimens, which vary with the percentage of cement of the investigated soils exhibited the highest resilient modulus values compared to those varying with the compacity.

7 Regression Analysis of the Resilient Modulus Test Results

7.1 Introduction

In recent years engineers have devoted considerable effort to determining the nonlinear stress–strain characteristics of pavement material. During the past few decades several constitutive models have been developed and used by pavement design engineers. These developments have provided powerful tools for research and design engineers to conduct pavement analysis in a more realistic manner. However stress and deformation or deformation analysis cannot be useful unless a correct constitutive equation that describes the actual behavior of material has been in the analysis. Each times a load passes in a pavement structure, the pavement rebounds less than it was deflected under load. After repeated loading and unloading sequences, each layer accumulates only a small amount of permanent deformation, with recoverable or resilient deformation. To explain this

Table 4 Bender element test-Longitudinal propagation

a

	Lat1-90	Lat1-95	Lat1-100	Lat3-90	Lat3-95	Lat3-100	Lat4-90	Lat4-95
Travel time	ts	ts	ts	ts	ts	ts	ts	ts
	486.2	343.4	425.8	438.3	509.9	465.8	392.8	434
	480.7	346.1	423	447.1	493.3	438.3	401	445
	478		425.8	427.3	513.2	458.1	403.8	
			431.3	427.3			412	
			425.8	443.8				
			425.8	436.1				
Average (ms)	481.63	344.75	426.25	436.65	505.47	454.07	402.40	439.50
Average (s)	0.000481633	0.00034475	0.00042625	0.00043665	0.000505467	0.000454067	0.0004024	0.0004395
Specimen length (mm)	173.7	177.8	171	181.5	179.6	174.8	180.3	183.1
Specimen diameter (mm)	102.36	103.19	103.82	102.55	102.55	103.06	103.19	102.36
Input protruded length (mm)	5	5	5	5	5	5	5	5
Output protruded length (mm)	5	5	5	5	5	5	5	5
Tip-to-tip distance (mm)	163.7	167.8	161	171.5	169.6	164.8	170.3	173.1
S-wave velocity (m/s)	339.89	486.73	377.71	392.76	335.53	362.94	423.21	393.86
Weight of specimen (kN)	0.0313	0.0314	0.0310	0.0316	0.0311	0.0306	0.0315	0.0312
Volume of specimen (m^3)	0.0014	0.0015	0.0014	0.0015	0.0015	0.0015	0.0015	0.0015
Specimen unit weight (kN/m^3)	21.92	21.10	21.40	21.08	20.94	20.98	20.89	20.71
Shear modulus (MPa)	258.14	509.60	311.15	331.52	240.36	281.78	381.44	327.46

b

	Lat4-100	Lat5-90	Lat5-95	Lat5-100	Lat6-90	Lat6-95	Lat6-100
Travel time	ts	ts	ts	ts	ts	ts	ts
	431	416.3	425.1	425.1	564.9	564	548.4
	434	421.8		427.3	570.4	553.9	
	434	427.3			568.2	542.9	
	442.3				570.4	557.2	
	434						
Average (ms)	435.06	421.80	425.10	426.20	568.48	554.50	548.40
Average (s)	0.00043506	0.0004218	0.0004251	0.0004262	0.000568475	0.0005545	0.0005484
Specimen length (mm)	181.5	172.7	174.7	173.5	174.1	165.5	172.9
Specimen diameter (mm)	102.49	102.24	102.62	102.24	103.12	106.11	104.52
Input protruded length (mm)	5	5	5	5	5	5	5

Table 4 continued

Output protruded length (mm)	5	5	5	5	5	5	5
Tip-to-tip distance (mm)	171.5	162.7	164.7	163.5	164.1	155.5	162.9
S-wave velocity (m/s)	394.20	385.73	387.44	383.62	288.67	280.43	297.05
Weight of specimen (kN)	0.0317	0.0314	0.0315	0.0316	0.0318	0.0314	0.0313
Volume of specimen (m3)	0.0015	0.0014	0.0014	0.0014	0.0015	0.0015	0.0015
Specimen unit weight (kN/m3)	21.14	22.15	21.82	22.17	21.84	21.46	21.11
Shear modulus (MPa)	334.86	335.87	333.87	332.65	185.51	172.03	189.91

Table 5 Test sequence AASHTOO T 292-97 (2000)

Conditioning	Sequence no.	Deviator stress (kPa)	Confining pressure (kPa)	No. of repetitions
Specimen conditioning	1	103	138	1,000
	2	69	138	50
	3	138	138	50
	4	207	138	50
	5	276	138	50
	6	69	103	50
	7	138	103	50
	8	207	103	50
	9	276	103	50
	10	34	69	50
Testing	11	69	69	50
	12	138	69	50
	13	207	69	50
	14	34	34	50
	15	69	34	50
	16	103	34	50
	17	34	21	50
	18	48	21	50
	19	62	21	50

behavior, researchers have used the concept of resilient modulus.

There are several models that were developed for the estimation of resilient modulus of subgrade soils and base/subbase materials.

Witczak and Uzan (1988) and Barksdale (1972) has shown that the resilient modulus of granular materials increase with increasing confining stress. The following bulk stress model is currently used by most pavement design engineers (Hicks and Monismith 1971; Shook et al. 1982):

$$M_{\mathrm{R}} = k_1 P_{\mathrm{a}} \left(\frac{\theta}{P_{\mathrm{a}}} \right)^{k_2}$$

in which

M_{R} = resilient modulus
θ = bulk stress at the peak of the loading or first stress invariant
= $\sigma_1 + \sigma_2 + \sigma_3$
= $3\sigma_{\mathrm{c}} + \Delta\sigma$, for standard triaxial compression loading
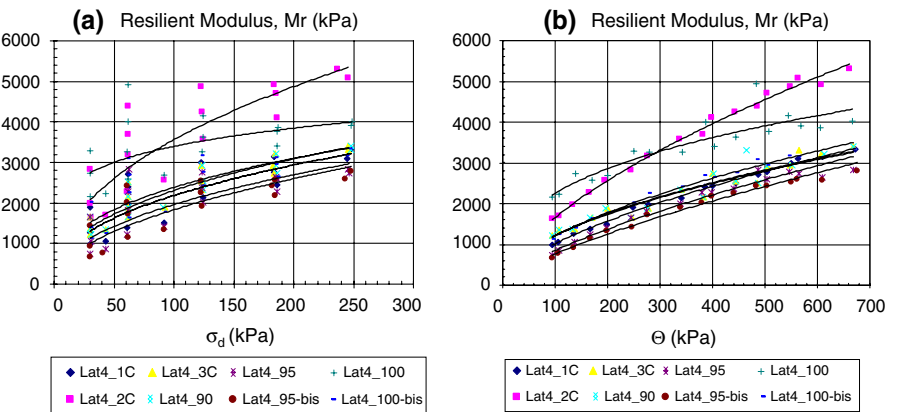k_1, k_2 = material and physical property parameters

Fig. 4 (**a**) k–σ_d model showing variation of moduli with deviator stress, Lat. 1 sample from 1% to 3% of cement added and from 90% to 100% OPM compacity. (**b**) k–Θ model showing variation of moduli with deviator stress, Lat. 1 sample from 1% to 3% of cement added and from 90% to 100% OPM compacity
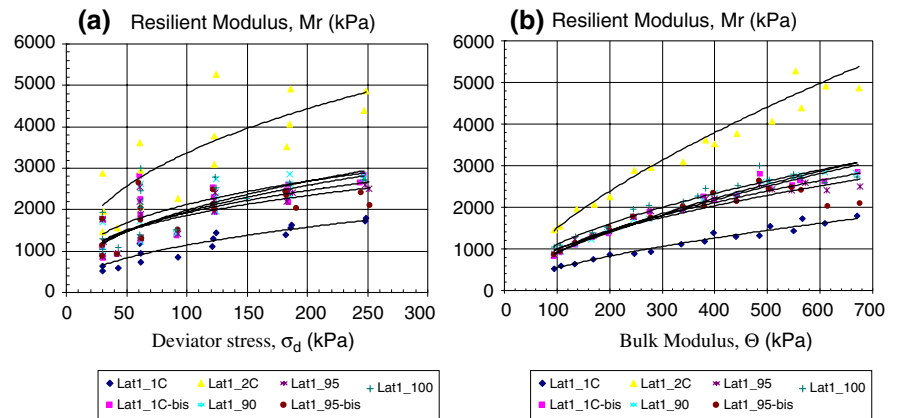
Fig. 5 (**a**) k–σ_d model showing variation of moduli with deviator stress, Lat. 3 sample from 1% to 3% of cement added and from 90% to 100% OPM compacity. (**b**) k–Θ model showing variation of moduli with deviator stress, Lat. 3 sample from 1% to 3% of cement added and from 90% to 100% OPM compacity
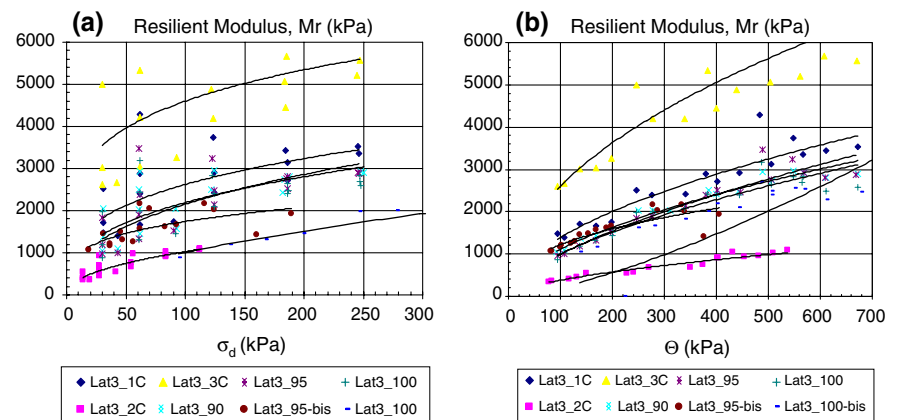
Fig. 6 (**a**) k–σ_d model showing variation of moduli with deviator stress, Lat. 4 sample from 1% to 3% of cement added and from 90% to 100% OPM compacity. (**b**) k–Θ model showing variation of moduli with deviator stress, Lat. 4 sample from 1% to 3% of cement added and from 90% to 100% OPM compacity

P_a = atmospheric pressure, expressed in the same unit as M_R and θ, used to make the constants independent of the units used

The main disadvantage of this model is that it does not adequately model the effect of deviator stress. May and Witczak (1981) suggested the following equation to describe the resilient modulus of granular materials:

$$M_R = K_1 k_1 \theta^{k_2}$$

where K_1 is a function of pavement structure, test load, and developed shear strain, and k_1, k_2 are constants.

Fig. 7 (**a**) k–σ_d model showing variation of moduli with deviator stress, Lat. 5 sample from 1% to 3% of cement added and from 90% to 100% OPM compacity. (**b**) k–Θ model showing variation of moduli with deviator stress, Lat. 5 sample from 1% to 3% of cement added and from 90% to 100% OPM compacity
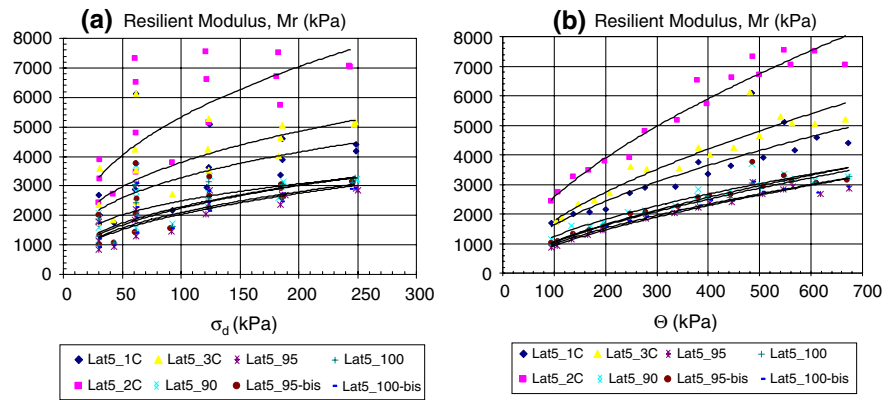
Fig. 8 (**a**) k–σ_d model showing variation of moduli with deviator stress, Lat. 6 sample from 1% to 3% of cement added and from 90% to 100% OPM compacity. (**b**) k–Θ model showing variation of moduli with deviator stress, Lat. 6 sample from 1% to 3% of cement added and from 90% to 100% OPM compacity
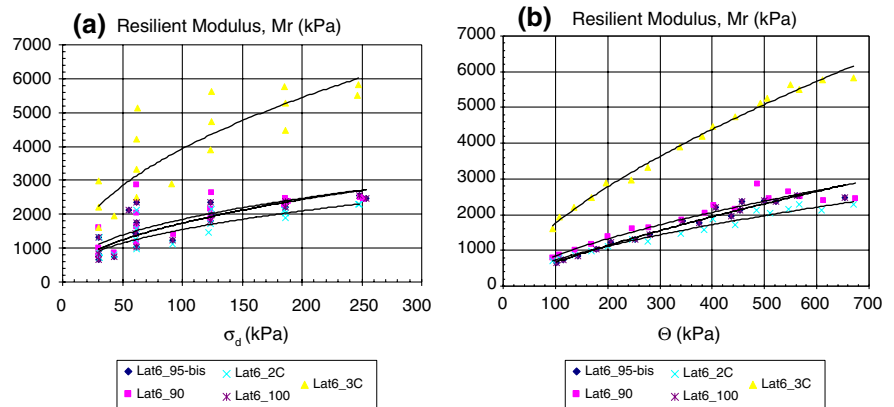
Uzan (1985) has demonstrated that the first equation expressed for granular material cannot adequately describe the nonlinear behavior of granular soils. In 1988, he suggested the equation below to describe the nonlinear behavior founded in repeated triaxial load tests, which was obtained from empirical observations. This model includes the influence of deviator stress on resilient modulus.

$$M_R = k_1 P_a \left(\frac{\theta}{P_a}\right)^{k_2} \left(\frac{\sigma_b}{P_a}\right)^{k_3}$$

where σ_d is the deviator stress ($\sigma_1 - \sigma_3$) and k_1, k_2, and k_3 are material constants.

A new "harmonized" resilient modulus test protocol is being developed through the NCHRP project 1-28A (NCHRP 2000) for implementation at the AASHTO 2002 pavement design guide. The new protocol uses the universal nonlinear model that is applicable for all types of subgrade soils and also for granular materials. The model is given by (NCHRP Project 1-37A 2002):

$$M_R = k_1 P_a \left(\frac{\sigma_b}{P_a}\right)^{k_2} \left(\frac{\tau_{oct}}{P_a} + 1\right)^{k_3}$$

where M_r is the resilient modulus, σ_d is the deviator stress, σ_b is the bulk stress (=$\sigma_1 + \sigma_2 + \sigma_3$), τ_{oct} is the octahedral shear stress, P_a is the atmospheric pressure (used to normalize M_r units), and k_1, k_2 and k_3 are material constants. This model is really close to the Andrei model (Andrei 1999) which makes differences from the use of the bulk stress compare to the model of the NCHRP Project using the deviator stress. The Andrei model is:

$$M_R = k_1 P_a \left(\frac{\theta}{P_a}\right)^{k_2} \left(\frac{\tau_{oct}}{P_a} + 1\right)^{k_3}.$$

7.2 Results

In this paper, the Uzan–Witczak universal model (Witczak and Uzan 1988), the Andrei model,

the k–Θ model ($M_R = k_3\theta^{k_4}$) and the power model ($M_R = k_1\sigma_d^{k_2}$) have been intensively use so as to find the best suitable model which can represent the relationship between resilient modulus and stress levels of lateritic soils used in this study. In order to achieve this, a linear regression analysis was conducted to evaluate the material constants k_1, k_2 and k_3.

Results of the statistical analysis are summarized in Table 6 (k–Θ model and the power model) and Table 7 (Uzan–Witczak model, Andrei model). The Uzan–Witczak universal nonlinear model and the Andrei model are preferred and presented so as to characterize the resilient modulus of the investigated soils. The predicted resilient moduli obtained from the power and k–Θ model gave a poor correlation to actual resilient moduli (Fig. 9a–e). The statistics given in Tables 6 and 7 provide evidence of better predictability in describing behavior of lateritic soils using the universal and the Andrei models than the power model. The k–Θ model gives good correlation but the fact that it's limited by only one variable (the bulk modulus). In this study, the two models as Andrei and Universal gave similar statistics and the choice had been make to evaluate the soil parameters with the Andrei parameters. The Andrei model is therefore more suitable to represent the relationship between resilient modulus and stress levels of granular lateritic soils.

Using the Andrei model, inspection of Table 7 indicates that the values of the material constants (k_1, k_2, and k_3) for the investigated soils vary significantly with samples state (from difference with the percentage of cement added) and not significantly when it is question of the state of compaction (from 90% of OPM to 100%). For example, when it is question of the percentage of cement added so as to stabilized the lateritic soil, the variation is very significant; so we get the following trend, with 1% of cement added, k_1 vary from 191 to 49 MPa, with 2% of cement 268 to 35.4 MPa and at least with 3% of cement, it increase from 347 to 35.4 MPa (Fig. 10a). k_1 vary from 258 to 103 MPa for soil samples at 100% OPM, 148–76.4 MPa at 95% and 135–102 MPa at 90% OPM (Fig. 10b).

The values of k_1 seem to be the most important material parameter and their variations have significant importance for the soil behavior estimation.

k_2 and k_3 change slowly in regard of with the variation of the compacity and significantly with the percentage of cement (Fig. 10c–e). For k_2, the variation is significant in regard of the percentage of cement added. At 1%, the mean is equal to –0.04 and k_2 vary from 0.060 to –0.100, at % from 0.080 to –0.110 and at 3%, from 0.020 to –0.100. k_3 seems to be less variable than the other sample's parameters. And from 1% to 3% of cement added, the variation is between 0.500 and 0.900, the minimum and the maximum is generally for 1% between 0.770 and 0.510, at 2% between 0.870 and 0.470 and at 3% between 0.810 and 0.470.

The trend of variation (of k_1 and k_2) seems to be less affected when it is question of the soil compacity and from 95% OPM to 100% OPM, k_2 is between –0.110 and 0 and k_2 from 0.510 to 0.760. At 90% OPM, the variation of k_2 and k_3 are more significant.

We can conclude right now that the most sensitive parameter, which can really change the soil's material parameter remains the percentage of cement which changes directly the soil rigidity. If we point out the soil compacity state, we can imagine than the AASHTO test procedure which began with 1,000 cycles of precondition cycling bring to the different soil at state which is somewhat nearly to the OPM. It that which gave not significant difference of the soil parameters when we point out the state of compacity.

Using the Uzan–Witczak universal nonlinear model, Inspection of Table 5 indicates that the values of the material constants (k_1, k_2, and k_3) for the investigated soils vary significantly with samples state (from difference with the percentage of cement added) and not significantly when it is question of the state of compaction (from 90% of OPM to 100%). For example, when it is question of the percentage of cement added so as to stabilized the lateritic soil, the variation is very significant; so we get the following trend, with 1% of cement added, k_1 vary from 191 to 49 MPa, with 2% of cement 268 to 35.4 MPa and at least with 3% of cement, it increase from 347 to 35.4 MPa (Fig. 11a). k_1 vary from 258 to 103 MPa for soil samples at 100% OPM, 148 to 76.4 MPa at 95% and 135 to 102 MPa at 90% OPM (Fig. 11b).

The values of k_1 seem to be the most important material parameter and their variations have significant importance for the soil behavior estimation.

k_2 and k_3 change slowly in regard of with the variation of the compacity and significantly with the percentage of cement (Fig. 11c–f). For k_2, the

	Power model $M_R = k_1 \sigma_d^{k_2}$			k–Θ model $M_R = k_3 \theta^{k_4}$		
Table 6 Variation of material constants with sample compacity and the percentage of cement for tested soils	k_1	k_2	r^2	k_3	k_4	r^2
Lat1_100	444.12	0.3397	0.71	93.47	0.5369	0.98
Lat1_95	374.58	0.3552	0.73	78.72	0.5493	0.98
Lat1_95′	406.07	0.3306	0.70	92.09	0.5169	0.94
Lat1_90	269.65	0.4336	0.79	50.08	0.6327	0.99
Lat1_2C	545.26	0.3956	0.66	68.96	0.6691	0.95
Lat1_1C	136.13	0.4623	0.93	32.73	0.6096	0.99
Lat1_1C′	297.80	0.4023	0.74	49.49	0.6314	0.99
Lat3_100	469.79	0.3251	0.68	65.49	0.5930	0.96
Lat3_95	329.08	0.4081	0.73	52.62	0.6380	0.98
Lat3_95′	535.25	0.2563	0.73	208.02	0.3844	0.88
Lat3_90	428.73	0.3545	0.73	86.77	0.5544	0.99
Lat3_3C	1,700.80	0.2161	0.45	287.61	0.4785	0.86
Lat3_2C	126.50	0.4546	0.85	25.60	0.5877	0.97
Lat3_1C	650.04	0.3030	0.63	123.3	0.5264	0.95
Lat4_100	1,497.40	0.1780	0.57	469.20	0.3411	0.93
Lat4_100′	418.52	0.3781	0.79	91.92	0.5594	0.99
Lat4_95	237.65	0.4584	0.76	35.36	0.6906	0.99
Lat4_95′	181.60	0.5023	0.81	28.59	0.7143	0.99
Lat4_90	335.65	0.3367	0.74	98.43	0.5350	0.99
Lat4_3C	332.64	0.4207	0.92	110.60	0.5201	0.97
Lat4_2C	445.96	0.4513	0.83	93.15	0.6258	0.99
Lat4_1C	306.64	0.4264	0.63	57.06	0.6259	0.99
Lat5_100	313.35	0.4273	0.79	57.48	0.6295	0.99
Lat5_100′	311.14	0.4147	0.77	56.50	0.6208	0.99
Lat5_95	285.76	0.4283	0.76	46.89	0.6486	0.99
Lat5_95′	362.42	0.4003	0.72	56.17	0.6375	0.98
Lat5_90	618.80	0.3023	0.67	95.81	0.5556	0.97
Lat5_3C	747.11	0.3529	0.68	103.07	0.6186	0.97
Lat5_2C	841.75	0.4008	0.76	162.24	0.5998	0.98
Lat5_1C	688.93	0.3386	0.64	111.00	0.5827	0.94
Lat6_100	186.46	0.4849	0.77	19.08	0.7714	0.99
Lat6_95′	186.46	0.4849	0.77	19.084	0.7714	0.99
Lat6_90	270.34	0.4176	0.75	44.54	0.6403	0.98
Lat6_3C	454.79	0.4685	0.83	84.84	0.6587	0.99
Lat6_2C	208.07	0.4361	0.81	41.87	0.6199	0.99

variation is significant in regard of the percentage of cement added. At 1%, the mean is equal to –0.676 and k_2 vary from 0.510 to 0.770, at 2% from 0.770 to 0.870 and at 3%, from 0.360 to 0.800. k_3 seems to be less variable than the other sample's parameters, this was observed when it was question of the Andrei model. And from 1% to 3% of cement added, the

variation of k_3 more significant and it is between –0.200 and 0.110 at 1%, at 2% between 0.140 and –0.030 and at 3% between 0.170 and –0.290.

The trend of variation (of k_1 and k_2) seems to be less affected when it is question of the soil compacity and from 90% OPM to 100% OPM, k_2 is between 0.510 and 0.750 and k_3 from –0.170 to 0.190.

Table 7 Variation of material constants with sample compacity and the percentage of cement for tested soils

| | Uzan–Witczak universal model (Witczak and Uzan 1988) $M_{\mathrm{R}} = k_1 \theta^{k_2} \sigma_{\mathrm{d}}^{k_3}$ | | | | Andrei model (Andrei, 1999) $M_{\mathrm{R}} = k_1 P_{\mathrm{a}} \left(\frac{\theta}{P_{\mathrm{a}}}\right)^{k_2} \left(\frac{\tau_{\mathrm{oct}}}{P_{\mathrm{a}}} + 1\right)^{k_3}$ | | | |
	k_1	k_2	k_3	r^2	k_4	k_5	k_6	r^2
Lat1_100	83	0.66	–0.13	0.982	12,285	–0.07	0.66	0.983
Lat1_95	72	0.63	–0.09	0.974	10,608	–0.05	0.64	0.975
Lat1_95′	85	0.6	–0.09	0.901	10,710	–0.05	0.6	0.902
Lat1_90	49	0.66	–0.03	0.994	9,412	–0.01	0.66	0.994
Lat1_2C	56	0.87	–0.21	0.954	17,915	–0.11	0.87	0.955
Lat1_1C	36	0.51	0.11	0.992	4,909	0.06	0.51	0.993
Lat1_1C′	45	0.73	–0.1	0.990	9,839	–0.05	0.73	0.990
Lat3_100	51	0.75	–0.15	0.955	11,183	–0.08	0.76	0.956
Lat3_95	47	0.74	–0.11	0.972	10,886	–0.06	0.75	0.972
Lat3_95′	152	0.58	–0.17	0.803	14,712	–0.11	0.62	0.818
Lat3_90	79	0.65	–0.1	0.991	12,051	–0.05	0.65	0.991
Lat3_3C	204	0.76	–0.29	0.836	34,724	–0.18	0.81	0.920
Lat3_2C	30	0.47	0.14	0.979	3,540	0.08	0.47	0.981
Lat3_1C	101	0.72	–0.2	0.970	16,384	–0.1	0.71	0.969
Lat4_100	393	0.51	–0.17	0.965	25,849	–0.09	0.51	0.967
Lat4_100′	89	0.59	–0.04	0.993	12,396	–0.02	0.59	0.994
Lat4_95	33	0.76	–0.07	0.984	9,051	–0.04	0.76	0.985
Lat4_95′	29	0.71	0.004	0.988	7,640	0.0001	0.71	0.988
Lat4_90	134	0.34	0.19	0.991	10,351	0.1	0.34	0.992
Lat4_3C	131	0.36	0.17	0.995	10,910	0.02	0.48	0.952
Lat4_2C	96	0.59	0.03	0.997	16,072	0.02	0.59	0.997
Lat4_1C	56	0.65	–0.03	0.997	10,373	–0.01	0.65	0.993
Lat5_100	56	0.66	–0.03	0.993	10,687	–0.02	0.66	0.993
Lat5_100′	54	0.67	–0.05	0.981	10,266	–0.03	0.67	0.981
Lat5_95	44	0.72	–0.08	0.981	9,890	–0.04	0.72	0.981
Lat5_95′	49	0.76	–0.13	0.980	11,807	–0.07	0.76	0.980
Lat5_90	81	0.68	–0.12	0.974	13,482	–0.06	0.68	0.974
Lat5_3C	81	0.8	–0.18	0.983	20,338	–0.1	0.8	0.984
Lat5_2C	154	0.65	–0.05	0.973	26,864	–0.03	0.65	0.973
Lat5_1C	91	0.77	–0.2	0.937	19,148	–0.1	0.77	0.938
Lat6_100	20	0.75	0.02	0.983	6,532	0.01	0.75	0.976
Lat6_95′	20	0.75	0.02	0.983	6,532	0.01	0.75	0.983
Lat6_90	41	0.72	–0.08	0.967	9,073	–0.04	0.72	0.968
Lat6_3C	87	0.63	0.03	0.993	17,191	0.01	0.64	0.993
Lat6_2C	42	0.61	0.01	0.981	7,171	0.01	0.61	0.981

We can conclude right now that the most sensitive parameter which can really change the soil's material parameter remains the percentage of cement which changes directly the soil rigidity. If we point out the soil compacity state, we can imagine than the AASHTOO test procedure which began with 1,000 cycles of precondition cycling bring to the different soil at state which is somewhat nearly to the OPM. It that which gave not significant difference of the soil parameters when we point out the state of compacity.

Fig. 9 (**a**) Actual resilient moduli versus predicted resilient moduli for Lat.1. (**b**) Actual resilient moduli versus predicted resilient moduli for Lat.3. (**c**) Actual resilient moduli versus predicted resilient moduli for Lat.4. (**d**) Actual resilient moduli versus predicted resilient moduli for Lat.5. (**e**) Actual resilient moduli versus predicted resilient moduli for Lat.6
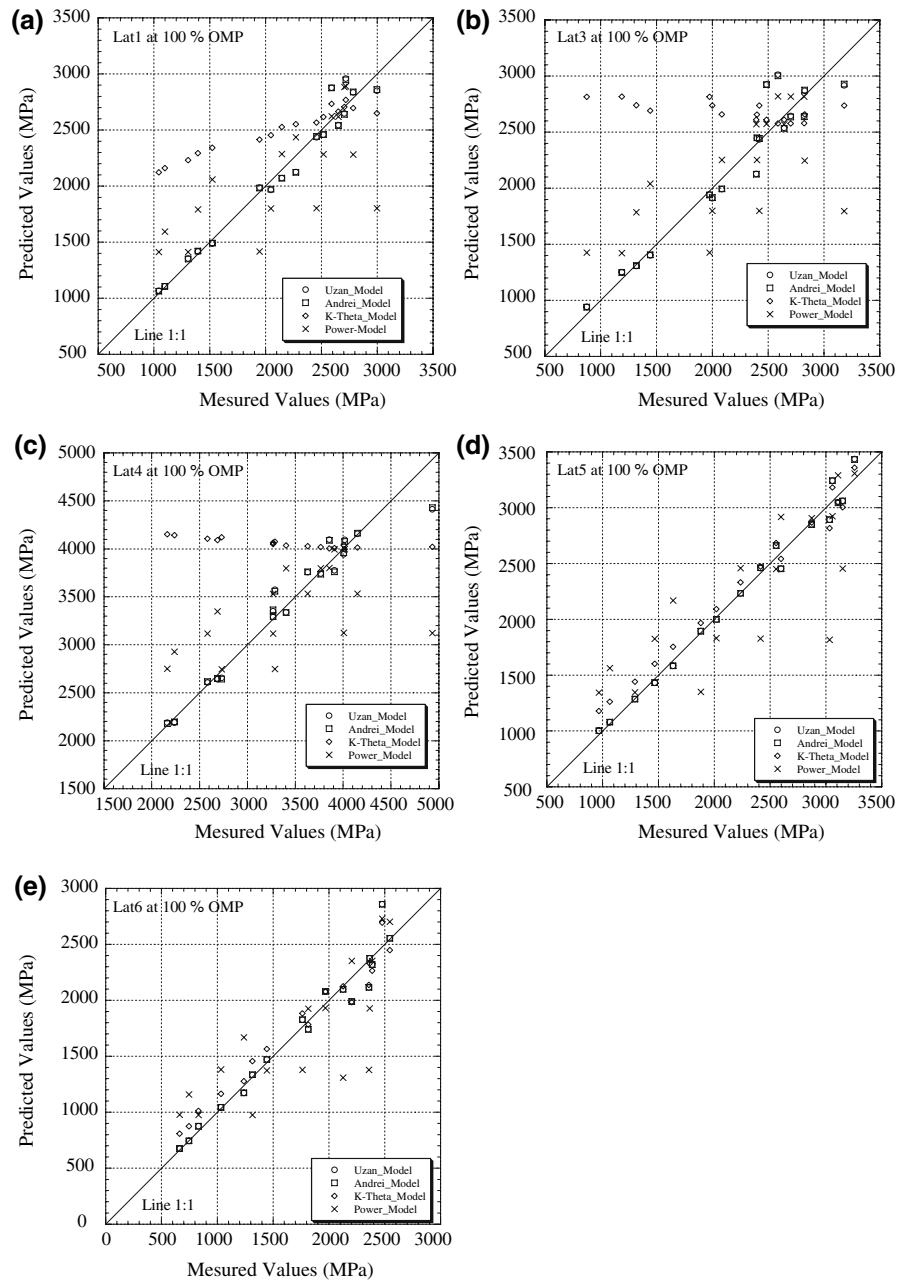

8 Conclusion

Repeated load triaxial test was conducted on different soils collected from different sites within Senegal. In order to investigate the effect of samples compacity and the percentage of cement added on resilient modulus, soil specimens with diameters of nearly 100 mm were considered. Soil specimens were subjected to resilient modulus test in accordance with AASHTO T 307. Test results showed that the resilient modulus for gravel lateritic soils is significantly affected by the percentage of cement added of the soil specimen tested. Soil specimens with 3% of cement exhibited the highest resilient modulus values while the specimens with the variation of the compacities exhibited the lowest values. The resilient

Fig. 10 (**a**) Variation of the material parameter k_1 with the percentage of cement added in the soil specimen. (**b**) Variation of the material parameter k_1 with t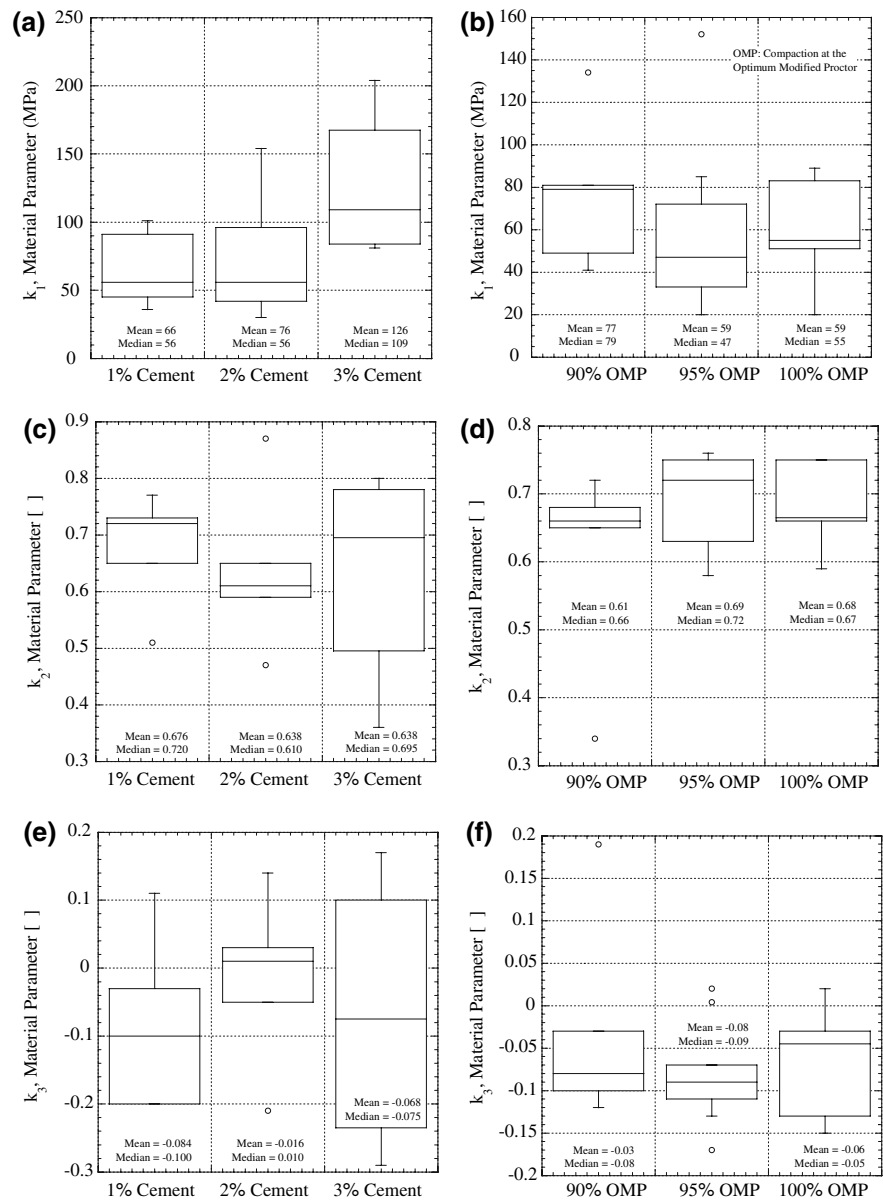he percentage of cement added in the soil specimen. (**c**) Variation of the material parameter k_2 with the percentage of cement added in the soil specimen. (**d**) Variation of the material parameter k_2 with the percentage of cement added in the soil specimen. (**e**) Variation of the material parameter k_3 with the percentage of cement added in the soil specimen. (**f**) Variation of the material parameter k_3 with the percentage of cement added in the soil specimen
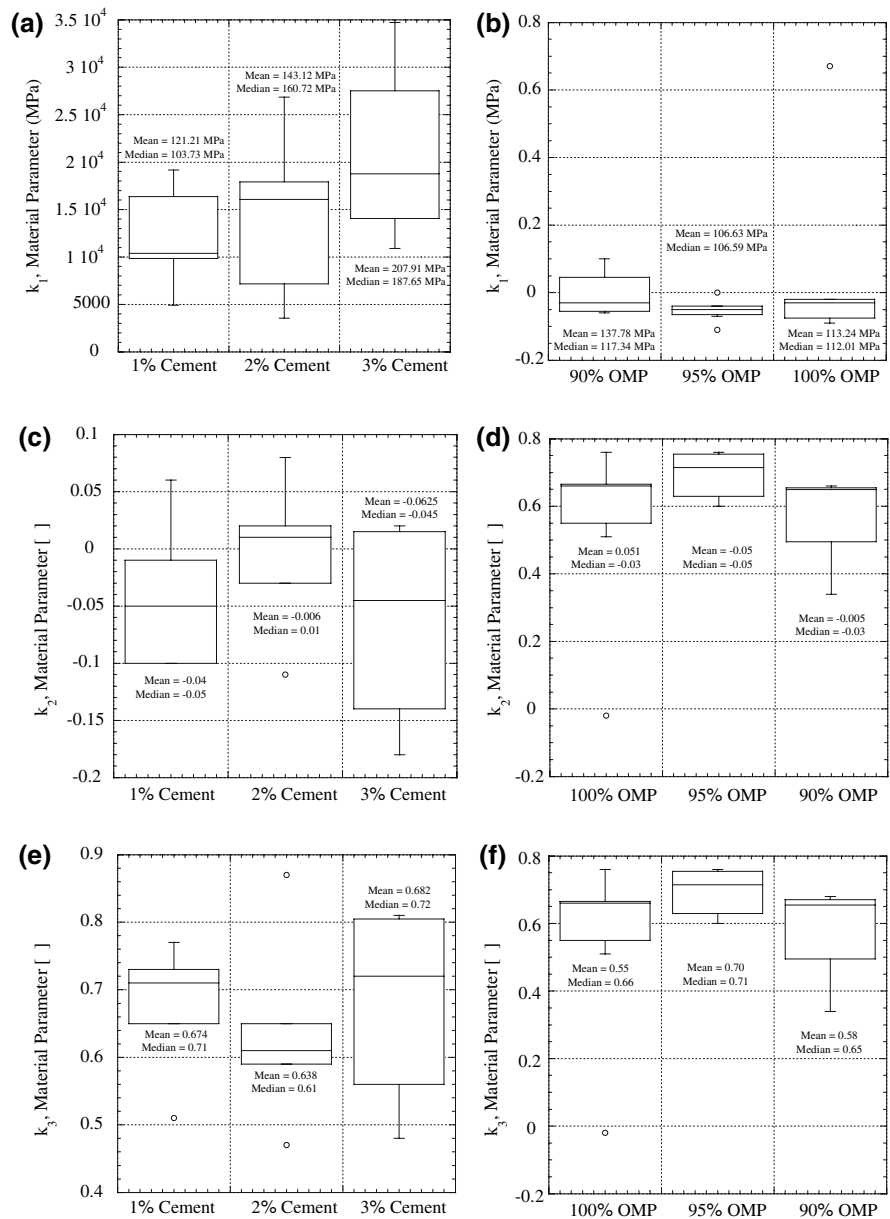
modulus variation with the percentage of cement was significant at low deviator stress levels and remains the same evolution with the increase of the deviator stress. Soil specimens with variation of the percentage of cement added exhibited the highest resilient modulus values while the specimens with variation of the compacity exhibited the lowest values. The resilient modulus variation seems to be independent of the level of stress. Results obtained in this research are no longer comparable to those obtained earlier for these kinds of materials, in Senegal. The correlation

between Young modulus with the CBR values to obtain a resilient modulus gives high characteristics, which are no longer justified for road design purposes.

Fig. 11 (**a**) Variation of the material parameter k_1 with the percentage of cement added in the soil specimen. (**b**) Variation of the material parameter k_1 with the percentage of cement added in the soil specimen. (**c**) Variation of the material parameter k_2 with the percentage of cement added in the soil specimen. (**d**) Variation of the material parameter k_2 with the percentage of cement added in the soil specimen. (**e**) Variation of the material parameter k_3 with the percentage of cement added in the soil specimen. (**f**) Variation of the material parameter k_3 with the percentage of cement added in the soil specimen

valuable input in this research project. The "*Entreprise Jean Lefebvre Senegal sa*" is greatly acknowledged for supporting the high-price shipping of lateritic materials from Senegal to Madison at Wisconsin (United States).

References

AASHTO (1986) Guide for Design of Pavement Structures. American Association of State Highway and Transportation Officials, Washington, DC

AASHTO (1993) Guide for Design of Pavement Structures. American Association of State Highway and Transportation Officials, Washington, DC

AASHTO T292-97 (2000) Test procedure for Resilient Modulus of Unbound Materials. American Association of State Highway and Transportation Officials, Washington, DC

AASHTO (2002) Guide for Design of Pavement Structures. American Association of State Highway and Transportation Officials, Washington, DC

AASHTO T 307 (2003) Determining the Resilient Modulus of Soils and Aggregate Materials. American Association of State Highway and Transportation Officials, Washington, DC

AASHTO T 99 (2001) Standard Method of Test for the Moisture-Density Relations of Soils. American Association of State Highway and Transportation Officials, Washington, DC

Andrei D (1999) Development of a Harmonized Test Protocol for the Resilient Modulus of Unbound Materials Used in Pavement Design, MS Thesis, University of Maryland—College Park

Barksdale RD (1972) Repeated load testing evaluation of base course materials, GHD research Project 7002, final report. FHWA, US Department of Transportation, 1972

BCEOM-CEBTP (1984) Manuel sur les routes dans les pays tropicaux et désertiques—Tome 1, 2 et 3. Ed. Min. Français Coop. Et Dév

Brown SF, Pappin JW (1981) Analysis of Pavements with Granular Bases, Transportation Research Record, Transportation Research Board, National Research Council, Washington, DC, pp 17–23

Chen HH, Marshek KM, Saraf CL (1986) Effects of truck tire contact pressure distribution on the design of flexible pavements: a three-dimensional finite element approach. Transport Res Rec 1095:72–78

Chen D-H, Zaman M, Laguros J, Soltani A (1995) Assessment of computer programs for analysis of flexible pavement structure. Transport Res Rec 1482:123–133

Dai S, Van Deusen D (1998) Field study of in situ subgrade soil response under flexible pavement. Transport Res Rec 1639:23–35

de Pont J, Thakur K, Pidwerbesky B, Steven B (2004) Validating a whole life pavement performance model. Transit New Zealand, CAPTIF Research Facility, 15

Dyvik R, Madshus C (1985) Lab measurements of G_{max} using bender elements. Proceedings of the advances in the art of testing soil under cyclic conditions, ASCE, Detroit, MI, 186–196

Fall M (1993) Identification et caractéristiques mécaniques de graveleux latéritiques du Sénégal. Application au domaine routier. Thèse de Doctorat en Génie Civil & Minier à l'INPL-ENSG, p 273, et Annexes;Nancy (France)

Fall M, Tisot J-P (1994) Specifications for road design using statistical data. An example of laterite or gravel lateritic soils from Senegal. Publié par l'AIGI (Géologie de l'Ingénieur), Bull. AIGI N°50 (Paris 1994)

Fall M, Tisot J-P (1995) Comportement mécanique à l'appareil de cisaillement de Casagrande de trois graveleux latéritiques compactés provenant du Sénégal Occidental. Publié par l'AIGI (Géologie de l'Ingénieur), Bull. AIGI N°52 (Paris 1995)

Fall M, Tisot J-P (1996) Undrained behaviour of compacted gravel lateritic soils from the western part of Senegal under monotonic and cyclic triaxial loading. Eng Geol 47(1997):71–87

Fall M, Senghor B, Lakhoune A (2002a) Analyse de la pratique du dimensionnement rationnel des structures de chaussées au Sénégal. Influence des paramètres d'entrée dans les codes de calcul pour le renforcement des chaussées. Annales du Batiment et des Travaux Publics, N° 1/02 (1/9)

Fall M, Paye F, Mbodji A (2002b) Current knowledge and research results for the design of flexible pavements in Senegal, EJGE, 2002

Fam M, Santamarina JC (1995) Study of geoprocesses with complementary wave measurements in an oedometer. Geotech Testing J 18(3):307–314

Fioravante V, Capoferri R (2001) On the use of multi-directional piezoelectric transducers in triaxial testings. Geotech Testing J 24(3):243–255

Hardy MSA, Cebon D (1993) Response of continuous pavements to moving dynamic loads. J Eng Mech, ASCE 119(9):1762–1780

Helwany S, Dyer J, Leidy J (1998) Finite-element analyses of flexible pavements. J Transport Eng, ASCE 124(5):491–499

Hicks RG, Monismith CL (1971) Factors influencing the relient properties of granular materials. Highway research record 345, Highway Research Board, Washington, DC pp 15–31

Hjelmstad KD, Taciroglu E (in press) Analysis and implementation of resilient modulus models for granular soils, J Eng Mech, ASCE

Huang YH (2004) Pavement analysis and design. Pearson Prentice Hall, Upper Saddle River, NJ

Jardine RJ, Potts DM, Fourie AB, Burland JB (1986) Studies of the influence of non-linear stress–strain characteristics in soil-structure interaction. Geotechnique 36(3):377–396

Jardine RJ, Potts DM (1988) Hutton tension platform foundation: an approach to the prediction of pile behavior. Geotechnique 38(2):231–252

Kim D-S, Stokoe KH II (1992) Characterization of resilient modulus of compacted subgrade soils using resonant column and torsional shear tests. Transport Res Rec 1369:83–91

Kim D-S, Kweon G-C, Lee K-H (1997) Alternative method of determining resilient modulus of compacted subgrade soils using free-free resonant column test. Transport Res Rec 1577:62–69

Lytton RL, Uzan J, Fernando EG, Roque R, Hiltunen DR, Stoffels SM (1993) Development and validation of performance prediction models and specifications for asphalt binders and paving mixtures. Report No. SHRP-A-357, Transportation Research Board, National Research Council, Washington, DC

Mancuso C, Vassallo R, d'Onofrio A (2002) Small strain behavior of a silty sand in controlled-suction resonant column-torsional shear tests. Can Geotech J 39(1):22–31

Marsh JG, Jewell RJ (1994) Vertical pavement strain as means of weighing vehicles. J Transport Eng, ASCE 120(4):617–632

May RW, Witczak MW (1981) Effective granular modulus to model pavement responses. In: Transportation research record 810, TRB, National Research Concil, Washington, DC, pp 1–9

NCHRP (2000) Harmonized test methods for laboratory determination of resilient modulus for flexible pavement design, vol 1, Unbound Granular Material, NCHRP Project 1–28a Draft Report, p 198

NCHRP Project 1–37A (2002) Summary of the 2002 AASHTO guide for the design of new and rehabilitated pavement structures. NCHRP, Washington, DC

NCHRP (2004) NCHRP Project 1–37A Design guide, mechanistic-empirical design of new and rehabilitated pavement structures, http://www.trb.org/mepdg/. NCHRP, Washington, DC

Pennington DS, Nash DFT, Lings ML (2001) Horizontally mounted bender elements for measuring anisotropic shear

moduli in triaxial clay specimens. Geotech Testing J 24(2):133–144

Pidwerbesky BD (1995) Strain response and performance of subgrades and flexible pavements under various loading conditions. Transport Res Rec 1482:87–93

Saleh MF, Steven B, Alabaster D (2003) Three-dimensional nonlinear finite element model for simulating pavement response: study at Canterbury accelerated pavement testing indoor facility, New Zealand. Transport Res Rec 1823:153–162

Sawangsuriya A, Edil TB, Bosscher PJ (2003) Relationship between soil stiffness gauge modulus and other test moduli for granular soils. Transport Res Rec 1849:3–10

Sawangsuriya A, Bosscher PJ, Edil TB (submitted) Application of the soil stiffness gauge in assessing small-strain stiffness of sand with different fabrics and densities. Geotech Testing J, ASTM

Sawangsuriya A, Biringen E, Fratta D, Bosscher PJ, Edil TB (2006) "Dimensionless limits for the collection and interpretation of wave propagation data in soils". ASCE Geotechnical Special Publication (GSP): "Site and Geomaterial Characterization". GeoShanghai Conference. Shanghai, China

Schwartz CW (2000) Effect of stress-dependent base layer on the superposition of two-dimensional flexible pavement solutions, proceedings, 2nd international conference on 3D finite elements for pavement analysis, design, and research, Charleston, WV, October, pp 329–354

Schwartz CW (2001) Implementation of a nonlinear resilient modulus constitutive model for unbound pavement materials, proceedings, 10th international conference on computer methods and advances in geomechanics, Tucson, AZ, January, pp 13851390

Seed HB, Idriss IM (1970) Soil moduli and damping factors for dynamic response analyses. Report EERC 70–10, Earthquake Engineering Research Center, University of California, Berkeley, CA

Shook JF, Finn FN, Witczak MW, Monismith CL (1982) Thickness design of asphalt pavement—the Asphalt Institute Methid. Presented at 5th international conference on the structural design of asphalt pavements, Delft, The Netherlands

Souto A, Hartikainen J, Özüdoğru K (1994) Measurement of dynamic parameters of road pavement materials by the bender element and resonant column tests. Geotechnique 44(3):519–526

Sun JI, Golesorkhi R, Seed HB (1988) Dynamic moduli and damping ratios for cohesive soils. Report EERC-88/15, Earthquake Engineering Research Center, University of California, Berkeley, CA

Tanyu BF, Kim WH, Edil TB, Benson CH (2003) Comparison of laboratory resilient modulus with back-calculated elastic moduli from large-scale model experiments and FWD tests on granular materials. Resilient Modulus Testing for Pavement Components, ASTM STP 1437, West Conshohocken, PA, pp 191–208

Tatsuoka F, Shibuya S (1991) Deformation characteristics of soils and rocks from field and laboratory tests. Proceedings of the 9th Asian regional conference on soil mech. and found. engrg., Bangkok, Thailand, vol 2. pp 101–170

Tatsuoka F, Siddiquee MS, Park CS, Sakamoto M, Abe F (1993) Modeling stress–strain relations of sand. Soils Found 33(2):60–81

Terzaghi K, Ralph BP (1948) Soil mechanics in engineering practice, Wiley, New York, The second edition by Ralph BP, 1967

Thomann TG, Hryciw RD (1990) Laboratory measurement of small strain shear modulus under K_o conditions. Geotech Testing J 13(2):97–105

Thompson MR (1990) NCHRP 1–26: Calibrated mechanistic structural analysis procedures for pavements. volume I—final report, prepared for the National Cooperative Highway Research Program, Transportation Research Board, National Research Council, Washington, DC, March

Thompson MR, Garg N (1999) Wheel load interaction: critical airport pavement responses, COE Report No. 7, Center of Excellence for Airport Pavement Research, Department of Civil Engineering, University of Illinois at Urbana-Champaign, July

Tutumluer E (1995) Predicting behavior of flexible pavements with granular bases, PhD dissertation, School of Civil and Environmental Engineering, Georgia Institute of Technology, Atlanta, GA

Tutumluer E, Little DN, Kim S-H (2003) Validated model for predicting field performance of aggregate base courses. Transp Res Rec 1837:41–49

Uzan J (1985) Characterization of granular material, transportation research record 1022, TRB, National Research Council, Washington, DC, pp 52–59

Uzan J (1991) SHRP Quarterly report: A-005 performance models and validation of test results. Quarter 2 of 4, of Year 2, Texas Transportation Institute, The Texas A&M University System, College Station, Texas, July 15

Vucetic M, Dobry R (1991) Effect of soil plasticity on cyclic response. J Geotech Eng, ASCE 117(1):89–107

Witczak MW, Uzan J (1988) The universal airport pavement design system. Report I of V: granular material characterization, Department of Civil Engineering, University of Maryland, College Park, MD

Yoder EJ, Witczak MW (1975) Principles of pavement design (2nd edn). Wiley, New York, NY

Zeng X, Ni B (1998) Application of bender elements in measuring G_{max} of sand under K_o condition. Geotech Testing J 21(3):251–263